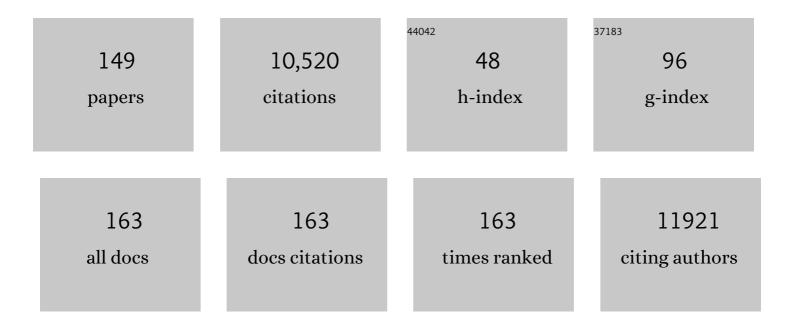
Markus C Wahl

List of Publications by Year in descending order

Source: https://exaly.com/author-pdf/3741744/publications.pdf Version: 2024-02-01



ΜΑΡΚΙΙSÂC WAHL

#	Article	IF	CITATIONS
1	The intrinsically disordered TSSC4 protein acts as a helicase inhibitor, placeholder and multi-interaction coordinator during snRNP assembly and recycling. Nucleic Acids Research, 2022, 50, 2938-2958.	6.5	11
2	CryoEM analysis of small plant biocatalysts at sub-2â€Ã resolution. Acta Crystallographica Section D: Structural Biology, 2022, 78, 113-123.	1.1	1
3	A nonâ€native Câ€terminal extension of the β' subunit compromises RNA polymerase and Rho functions. Molecular Microbiology, 2022, , .	1.2	0
4	A human kinase yeast array for the identification of kinases modulating phosphorylationâ€dependent protein–protein interactions. Molecular Systems Biology, 2022, 18, e10820.	3.2	9
5	A multi-factor trafficking site on the spliceosome remodeling enzyme BRR2 recruits C9ORF78 to regulate alternative splicing. Nature Communications, 2022, 13, 1132.	5.8	7
6	Steps toward translocation-independent RNA polymerase inactivation by terminator ATPase Ï• Science, 2021, 371, .	6.0	78
7	A skipping rope translocation mechanism in a widespread family of DNA repair helicases. Nucleic Acids Research, 2021, 49, 504-518.	6.5	7
8	Large-scale ratcheting in a bacterial DEAH/RHA-type RNA helicase that modulates antibiotics susceptibility. Proceedings of the National Academy of Sciences of the United States of America, 2021, 118, .	3.3	6
9	Long-range allostery mediates cooperative adenine nucleotide binding by the Ski2-like RNA helicase Brr2. Journal of Biological Chemistry, 2021, 297, 100829.	1.6	3
10	Transcription complexes as RNA chaperones. Transcription, 2021, 12, 126-155.	1.7	4
11	Characterization of the Brr2 RNA Helicase and Its Regulation by Other Spliceosomal Proteins Using Gel-Based U4/U6 Di-snRNA Binding and Unwinding Assays. Methods in Molecular Biology, 2021, 2209, 193-215.	0.4	0
12	Molecular Mechanism Underlying Inhibition of Intrinsic ATPase Activity in a Ski2-like RNA Helicase. Structure, 2020, 28, 236-243.e3.	1.6	12
13	Structure-Based Mechanisms of a Molecular RNA Polymerase/Chaperone Machine Required for Ribosome Biosynthesis. Molecular Cell, 2020, 79, 1024-1036.e5.	4.5	41
14	The interaction of DNA repair factors ASCC2 and ASCC3 is affected by somatic cancer mutations. Nature Communications, 2020, 11, 5535.	5.8	12
15	A Snu114–GTP–Prp8 module forms a relay station for efficient splicing in yeast. Nucleic Acids Research, 2020, 48, 4572-4584.	6.5	2
16	The inactive C-terminal cassette of the dual-cassette RNA helicase BRR2 both stimulates and inhibits the activity of the N-terminal helicase unit. Journal of Biological Chemistry, 2020, 295, 2097-2112.	1.6	12
17	A Conserved Kinase-Based Body-Temperature Sensor Globally Controls Alternative Splicing and Gene Expression. Molecular Cell, 2020, 78, 57-69.e4.	4.5	76
18	The δ subunit and NTPase HelD institute a two-pronged mechanism for RNA polymerase recycling. Nature Communications, 2020, 11, 6418.	5.8	32

#	Article	IF	CITATIONS
19	RIM-binding protein couples synaptic vesicle recruitment to release sites. Journal of Cell Biology, 2020, 219, .	2.3	26
20	Exploiting phage strategies to modulate bacterial transcription. Transcription, 2019, 10, 222-230.	1.7	6
21	Exon Inclusion Modulates Conformational Plasticity and Autoinhibition of the Intersectin 1 SH3A Domain. Structure, 2019, 27, 977-987.e5.	1.6	4
22	Structural basis for the function of SuhB as a transcription factor in ribosomal RNA synthesis. Nucleic Acids Research, 2019, 47, 6488-6503.	6.5	15
23	Increased versatility despite reduced molecular complexity: evolution, structure and function of metazoan splicing factor PRPF39. Nucleic Acids Research, 2019, 47, 5867-5879.	6.5	7
24	Structural Basis for the Action of an All-Purpose Transcription Anti-termination Factor. Molecular Cell, 2019, 74, 143-157.e5.	4.5	86
25	Phosphorylation of the Bruchpilot N-terminus unlocks axonal transport of active zone building blocks. Journal of Cell Science, 2019, 132, .	1.2	5
26	Intramolecular domain dynamics regulate synaptic MAGUK protein interactions. ELife, 2019, 8, .	2.8	33
27	The aldehyde dehydrogenase AldA contributes to the hypochlorite defense and is redox-controlled by protein S-bacillithiolation in Staphylococcus aureus. Redox Biology, 2018, 15, 557-568.	3.9	38
28	Intrinsically Disordered Protein Ntr2 Modulates the Spliceosomal RNA Helicase Brr2. Biophysical Journal, 2018, 114, 788-799.	0.2	15
29	Protein <i>S</i> -Bacillithiolation Functions in Thiol Protection and Redox Regulation of the Glyceraldehyde-3-Phosphate Dehydrogenase Gap in <i>Staphylococcus aureus</i> Under Hypochlorite Stress. Antioxidants and Redox Signaling, 2018, 28, 410-430.	2.5	58
30	Redox-Sensing Under Hypochlorite Stress and Infection Conditions by the Rrf2-Family Repressor HypR in <i>Staphylococcus aureus</i> . Antioxidants and Redox Signaling, 2018, 29, 615-636.	2.5	51
31	Crystal Structure of the Escherichia coli DExH-Box NTPase HrpB. Structure, 2018, 26, 1462-1473.e4.	1.6	10
32	Molecular insights into antibiotic resistance - how a binding protein traps albicidin. Nature Communications, 2018, 9, 3095.	5.8	32
33	Molecular principles underlying dual RNA specificity in the Drosophila SNF protein. Nature Communications, 2018, 9, 2220.	5.8	7
34	Bacterial Polysaccharide Specificity of the Pattern Recognition Receptor Langerin Is Highly Species-dependent. Journal of Biological Chemistry, 2017, 292, 862-871.	1.6	33
35	Internal Dynamics of the 3-Pyrroline- <i>N</i> -Oxide Ring in Spin-Labeled Proteins. Journal of Physical Chemistry Letters, 2017, 8, 1113-1117.	2.1	2
36	Structural basis for λN-dependent processive transcription antitermination. Nature Microbiology, 2017, 2, 17062.	5.9	58

#	Article	IF	CITATIONS
37	Human MFAP1 is a cryptic ortholog of the Saccharomyces cerevisiae Spp381 splicing factor. BMC Evolutionary Biology, 2017, 17, 91.	3.2	13
38	Interplay of <i>cis</i> - and <i>trans</i> -regulatory mechanisms in the spliceosomal RNA helicase Brr2. Cell Cycle, 2017, 16, 100-112.	1.3	28
39	A new role for FBP21 as regulator of Brr2 helicase activity. Nucleic Acids Research, 2017, 45, 7922-7937.	6.5	24
40	Structural Basis for the Functional Coupling of the Alternative Splicing Factors Smu1 and RED. Structure, 2016, 24, 762-773.	1.6	25
41	Tracking Transient Conformational States of T4 Lysozyme at Room Temperature Combining X-ray Crystallography and Site-Directed Spin Labeling. Journal of the American Chemical Society, 2016, 138, 12868-12875.	6.6	13
42	Active zone scaffolds differentially accumulate Unc13 isoforms to tune Ca2+ channel–vesicle coupling. Nature Neuroscience, 2016, 19, 1311-1320.	7.1	166
43	The right pick: structural basis of snRNA selection by Gemin5. Genes and Development, 2016, 30, 2341-2344.	2.7	11
44	MPP2 is a postsynaptic MAGUK scaffold protein that links SynCAM1 cell adhesion molecules to core components of the postsynaptic density. Scientific Reports, 2016, 6, 35283.	1.6	24
45	Scaffolding in the Spliceosome via Single α Helices. Structure, 2016, 24, 1972-1983.	1.6	24
46	Functions and regulation of the Brr2 RNA helicase during splicing. Cell Cycle, 2016, 15, 3362-3377.	1.3	37
47	Substrate-assisted mechanism of RNP disruption by the spliceosomal Brr2 RNA helicase. Proceedings of the United States of America, 2016, 113, 7798-7803.	3.3	21
48	Multiple protein–protein interactions converging on the Prp38 protein during activation of the human spliceosome. Rna, 2016, 22, 265-277.	1.6	24
49	SnapShot: Spliceosome Dynamics I. Cell, 2015, 161, 1474-1474.e1.	13.5	66
50	The large N-terminal region of the Brr2 RNA helicase guides productive spliceosome activation. Genes and Development, 2015, 29, 2576-2587.	2.7	54
51	Fluorine teams up with water to restore inhibitor activity to mutant BPTI. Chemical Science, 2015, 6, 5246-5254.	3.7	32
52	SnapShot: Spliceosome Dynamics III. Cell, 2015, 162, 690-690.e1.	13.5	46
53	A noncanonical PWI domain in the N-terminal helicase-associated region of the spliceosomal Brr2 protein. Acta Crystallographica Section D: Biological Crystallography, 2015, 71, 762-771.	2.5	29
54	SnapShot: Spliceosome Dynamics II. Cell, 2015, 162, 456-456.e1.	13.5	25

#	Article	IF	CITATIONS
55	Structures of <i>Drosophila melanogaster</i> Rab2 and Rab3 bound to GMPPNP. Acta Crystallographica Section F, Structural Biology Communications, 2015, 71, 34-40.	0.4	5
56	Presynaptic spinophilin tunes neurexin signalling to control active zone architecture and function. Nature Communications, 2015, 6, 8362.	5.8	51
57	A high affinity RIM-binding protein/Aplip1 interaction prevents the formation of ectopic axonal active zones. ELife, 2015, 4, .	2.8	26
58	A composite double-/single-stranded RNA-binding region in protein Prp3 supports tri-snRNP stability and splicing. ELife, 2015, 4, e07320.	2.8	29
59	Novel regulatory principles of the spliceosomal Brr2 RNA helicase and links to retinal disease in humans. RNA Biology, 2014, 11, 298-312.	1.5	39
60	Cooperative structure of the heterotrimeric pre-mRNA retention and splicing complex. Nature Structural and Molecular Biology, 2014, 21, 911-918.	3.6	28
61	Entrapment of DNA in an intersubunit tunnel system of a single-stranded DNA-binding protein. Nucleic Acids Research, 2014, 42, 6698-6708.	6.5	15
62	Structure and evolution of the spliceosomal peptidyl-prolyl <i>cis</i> – <i>trans</i> isomerase Cwc27. Acta Crystallographica Section D: Biological Crystallography, 2014, 70, 3110-3123.	2.5	19
63	Drep-2 is a novel synaptic protein important for learning and memory. ELife, 2014, 3, .	2.8	39
64	An Autoinhibited State in the Structure of Thermotoga maritima NusG. Structure, 2013, 21, 365-375.	1.6	16
65	Inhibition of RNA Helicase Brr2 by the C-Terminal Tail of the Spliceosomal Protein Prp8. Science, 2013, 341, 80-84.	6.0	122
66	Structural basis for dual roles of Aar2p in U5 snRNP assembly. Genes and Development, 2013, 27, 525-540.	2.7	26
67	The Prp8 RNase H-like domain inhibits Brr2-mediated U4/U6 snRNA unwinding by blocking Brr2 loading onto the U4 snRNA. Genes and Development, 2012, 26, 2422-2434.	2.7	65
68	Structural basis for functional cooperation between tandem helicase cassettes in Brr2-mediated remodeling of the spliceosome. Proceedings of the National Academy of Sciences of the United States of America, 2012, 109, 17418-17423.	3.3	85
69	Structure determination by multiple-wavelength anomalous dispersion (MAD) at the Prâ€ <i>L</i> _{III} edge. Acta Crystallographica Section F: Structural Biology Communications, 2012, 68, 981-984.	0.7	3
70	A reversibly photoswitchable GFP-like protein with fluorescence excitation decoupled from switching. Nature Biotechnology, 2011, 29, 942-947.	9.4	254
71	Common Design Principles in the Spliceosomal RNA Helicase Brr2 and in the Hel308 DNA Helicase. Molecular Cell, 2011, 41, 366.	4.5	0
72	Mass-spectrometric analysis of proteins cross-linked to 4-thio-uracil- and 5-bromo-uracil-substituted RNA. International Journal of Mass Spectrometry, 2011, 304, 184-194.	0.7	29

#	Article	IF	CITATIONS
73	Mechanism for Aar2p function as a U5 snRNP assembly factor. Genes and Development, 2011, 25, 1601-1612.	2.7	35
74	Structural basis for the dual U4 and U4atac snRNA-binding specificity of spliceosomal protein hPrp31. Rna, 2011, 17, 1655-1663.	1.6	14
75	Primordial neurosecretory apparatus identified in the choanoflagellate <i>Monosiga brevicollis</i> . Proceedings of the National Academy of Sciences of the United States of America, 2011, 108, 15264-15269.	3.3	74
76	Crystal Structure Analysis Reveals Functional Flexibility in the Selenocysteine-Specific tRNA from Mouse. PLoS ONE, 2011, 6, e20032.	1.1	17
77	Functional organization of the Sm core in the crystal structure of human U1 snRNP. EMBO Journal, 2010, 29, 4172-4184.	3.5	115
78	Fine tuning of the E. coli NusB:NusE complex affinity to BoxA RNA is required for processive antitermination. Nucleic Acids Research, 2010, 38, 314-326.	6.5	22
79	A novel Nop5–sRNA interaction that is required for efficient archaeal box C/D sRNP formation. Rna, 2010, 16, 2341-2348.	1.6	15
80	Molecular Basis of the Light-driven Switching of the Photochromic Fluorescent Protein Padron. Journal of Biological Chemistry, 2010, 285, 14603-14609.	1.6	65
81	Evolution of CASK into a Mg ²⁺ -Sensitive Kinase. Science Signaling, 2010, 3, ra33.	1.6	48
82	A NusE:NusG Complex Links Transcription and Translation. Science, 2010, 328, 501-504.	6.0	294
83	The Crystal Structure of PPIL1 Bound to Cyclosporine A Suggests a Binding Mode for a Linear Epitope of the SKIP Protein. PLoS ONE, 2010, 5, e10013.	1.1	23
84	Functional stabilization of an RNA recognition motif by a noncanonical N-terminal expansion. Rna, 2009, 15, 1305-1313.	1.6	16
85	The Thermodynamic Influence of Trapped Water Molecules on a Protein–Ligand Interaction. Angewandte Chemie - International Edition, 2009, 48, 5207-5210.	7.2	36
86	Helical extension of the neuronal SNARE complex into the membrane. Nature, 2009, 460, 525-528.	13.7	368
87	The Spliceosome: Design Principles of a Dynamic RNP Machine. Cell, 2009, 136, 701-718.	13.5	2,190
88	Crystal Structure of the Pml1p Subunit of the Yeast Precursor mRNA Retention and Splicing Complex. Journal of Molecular Biology, 2009, 385, 531-541.	2.0	19
89	Common Design Principles in the Spliceosomal RNA Helicase Brr2 and in the Hel308 DNA Helicase. Molecular Cell, 2009, 35, 454-466.	4.5	83
90	The origin of eubacteria with three L7/L12 protein dimers in the ribosome. Doklady Biochemistry and Biophysics, 2008, 422, 257-260.	0.3	1

#	Article	IF	CITATIONS
91	Structure and function of an RNase H domain at the heart of the spliceosome. EMBO Journal, 2008, 27, 2929-2940.	3.5	91
92	Structural and Functional Analysis of the E. coli NusB-S10 Transcription Antitermination Complex. Molecular Cell, 2008, 32, 791-802.	4.5	95
93	CASK Functions as a Mg2+-Independent Neurexin Kinase. Cell, 2008, 133, 328-339.	13.5	246
94	Structure and Catalytic Mechanism of Eukaryotic Selenocysteine Synthase. Journal of Biological Chemistry, 2008, 283, 5849-5865.	1.6	49
95	An Unusual RNA Recognition Motif Acts as a Scaffold for Multiple Proteins in the Pre-mRNA Retention and Splicing Complex. Journal of Biological Chemistry, 2008, 283, 32317-32327.	1.6	22
96	1.8 Ã bright-state structure of the reversibly switchable fluorescent protein Dronpa guides the generation of fast switching variants. Biochemical Journal, 2007, 402, 35-42.	1.7	228
97	Structural basis for reversible photoswitching in Dronpa. Proceedings of the National Academy of Sciences of the United States of America, 2007, 104, 13005-13009.	3.3	250
98	Towards understanding selenocysteine incorporation into bacterial proteins. Biological Chemistry, 2007, 388, 1061-1067.	1.2	16
99	Structure of a Multipartite Protein-Protein Interaction Domain in Splicing Factor Prp8 and Its Link to Retinitis Pigmentosa. Molecular Cell, 2007, 25, 615-624.	4.5	119
100	Binding of the Human Prp31 Nop Domain to a Composite RNA-Protein Platform in U4 snRNP. Science, 2007, 316, 115-120.	6.0	125
101	Conformational switches in winged-helix domains 1 and 2 of bacterial translation elongation factor SelB. Acta Crystallographica Section D: Biological Crystallography, 2007, 63, 1075-1081.	2.5	Ο
102	Early endosomal SNAREs form a structurally conserved SNARE complex and fuse liposomes with multiple topologies. EMBO Journal, 2007, 26, 9-18.	3.5	71
103	Mitogen-activated protein kinases interacting kinases are autoinhibited by a reprogrammed activation segment. EMBO Journal, 2006, 25, 4020-4032.	3.5	71
104	Biochemical and NMR analyses of an SF3b155-p14-U2AF-RNA interaction network involved in branch point definition during pre-mRNA splicing. Rna, 2006, 12, 410-425.	1.6	69
105	Crystal Structures of the Mnk2 Kinase Domain Reveal an Inhibitory Conformation and a Zinc Binding Site. Structure, 2005, 13, 1559-1568.	1.6	57
106	Structures of Escherichia coli NAD Synthetase with Substrates and Products Reveal Mechanistic Rearrangements. Journal of Biological Chemistry, 2005, 280, 15131-15140.	1.6	34
107	Structure and mechanism of the reversible photoswitch of a fluorescent protein. Proceedings of the National Academy of Sciences of the United States of America, 2005, 102, 13070-13074.	3.3	253
108	Structural and Functional Investigation of a Putative Archaeal Selenocysteine Synthaseâ€,‡. Biochemistry, 2005, 44, 13315-13327.	1.2	297

#	Article	IF	CITATIONS
109	Oligomeric State and Mode of Self-Association ofThermotoga maritimaRibosomal Stalk Protein L12 in Solutionâ€. Biochemistry, 2005, 44, 3298-3305.	1.2	6
110	Comparative Structural Analysis of Oxidized and Reduced Thioredoxin from Drosophila melanogaster. Journal of Molecular Biology, 2005, 345, 1119-1130.	2.0	50
111	Structural Basis for the Function of the Ribosomal L7/12 Stalk in Factor Binding and GTPase Activation. Cell, 2005, 121, 991-1004.	13.5	354
112	Structural basis for the interaction of Escherichia coli NusA with protein N of phage Â. Proceedings of the United States of America, 2004, 101, 13762-13767.	3.3	28
113	Crystal structures of the antitermination factor NusB from Thermotoga maritima and implications for RNA binding. Biochemical Journal, 2004, 383, 419-428.	1.7	11
114	The Zinc Finger-Associated Domain of the Drosophila Transcription Factor Grauzone Is a Novel Zinc-Coordinating Protein-Protein Interaction Module. Structure, 2003, 11, 1393-1402.	1.6	47
115	Determinants of Enzymatic Specificity in the Cys-Met-Metabolism PLP-Dependent Enzyme Family: Crystal Structure of Cystathionine γ-Lyase from Yeast and Intrafamiliar Structure Comparison. Biological Chemistry, 2003, 384, 373-86.	1.2	94
116	Crystal Structure of a Complex Between Human Spliceosomal Cyclophilin H and a U4/U6 snRNP-60K Peptide. Journal of Molecular Biology, 2003, 331, 45-56.	2.0	46
117	The extended loops of ribosomal proteins L4 and L22 are not required for ribosome assembly or L4-mediated autogenous control. Rna, 2003, 9, 1188-1197.	1.6	43
118	Elevated plasma total homocysteine in severe methionine adenosyltransferase I/III deficiency. Metabolism: Clinical and Experimental, 2002, 51, 981-988.	1.5	68
119	Comparative anatomy of a regulatory ribosomal protein. Biochimie, 2002, 84, 731-743.	1.3	5
120	Crystal structures of transcription factor NusG in light of its nucleic acid- and protein-binding activities. EMBO Journal, 2002, 21, 4641-4653.	3.5	102
121	Structure and Function of the Acidic Ribosomal Stalk Proteins. Current Protein and Peptide Science, 2002, 3, 93-106.	0.7	94
122	An Extended RNA Binding Surface through Arrayed S1 and KH Domains in Transcription Factor NusA. Molecular Cell, 2001, 7, 1177-1189.	4.5	87
123	The Polypeptide Tunnel System in the Ribosome and Its Gating in Erythromycin Resistance Mutants of L4 and L22. Molecular Cell, 2001, 8, 181-188.	4.5	187
124	B-form to A-form conversion by a 3'-terminal ribose: crystal structure of the chimera d(CCACTAGTG)r(G). Nucleic Acids Research, 2000, 28, 4356-4363.	6.5	35
125	Expression, purification, crystallization and preliminary X-ray diffraction studies of bacterial and archaeal L4 ribosomal proteins. Acta Crystallographica Section D: Biological Crystallography, 2000, 56, 645-647.	2.5	1
126	Flexibility, conformational diversity and two dimerization modes in complexes of ribosomal protein L12. EMBO Journal, 2000, 19, 174-186.	3.5	84

#	Article	IF	CITATIONS
127	Crystal structure of ribosomal protein L4 shows RNA-binding sites for ribosome incorporation and feedback control of the S10 operon. EMBO Journal, 2000, 19, 807-818.	3.5	43
128	Structural Investigations of the Highly Flexible Recombinant Ribosomal Protein L12 from Thermotoga maritima. Biological Chemistry, 2000, 381, 221-9.	1.2	3
129	Crystal structure of an RNA duplex r(GGGCGCUCC)2 with non-adjacent G{middle dot}U base pairs. Nucleic Acids Research, 1999, 27, 2196-2201.	6.5	25
130	Cloning, Purification and Characterisation of Cystathionine Î ³ -Synthase from Nicotiana tabacum. Biological Chemistry, 1999, 380, 1237-42.	1.2	19
131	Kinetics and Inhibition of Recombinant Human Cystathionine Î ³ -Lyase. Journal of Biological Chemistry, 1999, 274, 12675-12684.	1.6	98
132	Structure of the side-by-side binding of distamycin to d(GTATATAC)2. Acta Crystallographica Section D: Biological Crystallography, 1999, 55, 602-609.	2.5	32
133	Crystal structure of Escherichia coli cystathionine Î ³ -synthase at 1.5 Ã resolution. EMBO Journal, 1998, 17, 6827-6838.	3.5	90
134	Cloning, purification, crystallization, and preliminary X-ray diffraction analysis of cystathionine γ-synthase fromE. coli. FEBS Letters, 1997, 414, 492-496.	1.3	12
135	Crystal structure of an alternating octamer r(GUAUGUA)dC with adjacent G·U wobble pairs. Journal of Molecular Biology, 1997, 267, 1149-1156.	2.0	53
136	C_H…O hydrogen bonding in biology. Trends in Biochemical Sciences, 1997, 22, 97-102.	3.7	315
137	Crystal structures of A-DNA duplexes. , 1997, 44, 45-63.		99
138	Crystal structure of the B-DNA hexamer d(CTCGAG): model for an A-to-B transition. Biophysical Journal, 1996, 70, 2857-2866.	0.2	26
139	Structure of the Purine–Pyrimidine Alternating RNA Double Helix, r(GUAUAUA)d(C), with a 3'-Terminal Deoxy Residue. Acta Crystallographica Section D: Biological Crystallography, 1996, 52, 655-667.	2.5	23
140	RNA – Synthesis, Purification and Crystallization. Acta Crystallographica Section D: Biological Crystallography, 1996, 52, 668-675.	2.5	10
141	The structure of r(UUCGCG) has a 5′-UU-overhang exhibiting Hoogsteen-like trans U•U base pairs. Nature Structural Biology, 1996, 3, 24-31.	9.7	95
142	New crystal structures of nucleic acids and their complexes. Current Opinion in Structural Biology, 1995, 5, 282-295.	2.6	28
143	Broadband axialization in an ion cyclotron resonance ion trap. Journal of Chemical Physics, 1994, 100, 6137-6140.	1.2	35
144	Shrink-wrapping an ion cloud for high-performance Fourier transform ion cyclotron resonance mass spectrometry. Chemical Reviews, 1994, 94, 2161-2182.	23.0	118

#	Article	IF	CITATIONS
145	MS/MS with High Detection Efficiency and Mass Resolving Power for Product Ions in Fourier Transform Ion Cyclotron Resonance Mass Spectrometry. Analytical Chemistry, 1994, 66, 1363-1367.	3.2	49
146	Enhanced mass resolving power, sensitivity, and selectivity in laser desorption Fourier transform ion cyclotron resonance mass spectrometry by ion axialization and cooling. Analytical Chemistry, 1993, 65, 1753-1757.	3.2	78
147	Elimination of frequency drift from Fourier transform ion cyclotron resonance mass spectra by digital quadrature heterodyning: ultrahigh mass resolving power for laser-desorbed molecules. Analytical Chemistry, 1993, 65, 3647-3653.	3.2	56
148	Thin gold film-assisted laser desorption/ionization Fourier transform ion cyclotron resonance mass spectrometry of biomolecules. Analytical Chemistry, 1993, 65, 3669-3676.	3.2	25
149	Molecular Mechanisms of an All-Purpose Transcription Anti-Termination Factor. SSRN Electronic Journal, O, , .	0.4	0